Electronic Supplementary Material (ESI) for Catalysis Science & Technology.

Supporting information

Nitrogen functionalized reduced graphene oxide as carbocatalysts with enhanced activity for polyaromatic hydrocarbons hydrogenation

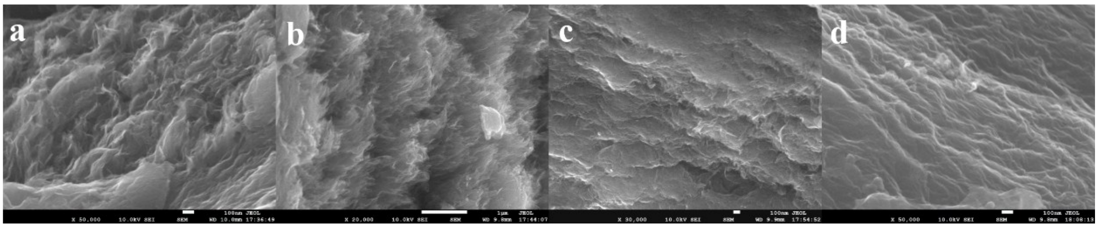

Figure S1. The SEM images of A-rGO650 (a), A-rGO800 (b), A-rGO1000 (c), and A-rGO1100 (d).

Table S1. The elements concentrations derived from EDX.

samples	C (at%)	N (at%)	O (at%)
A-rGO450	86.38	7.75	5.87
A-rGO650	87.89	6.95	5.16
A-rGO800	91.98	4.73	3.29
A-rGO900	93.23	3.99	2.78
A-rGO1000	96.89	2.27	0.84
A-rGO1100	97.97	1.56	0.47

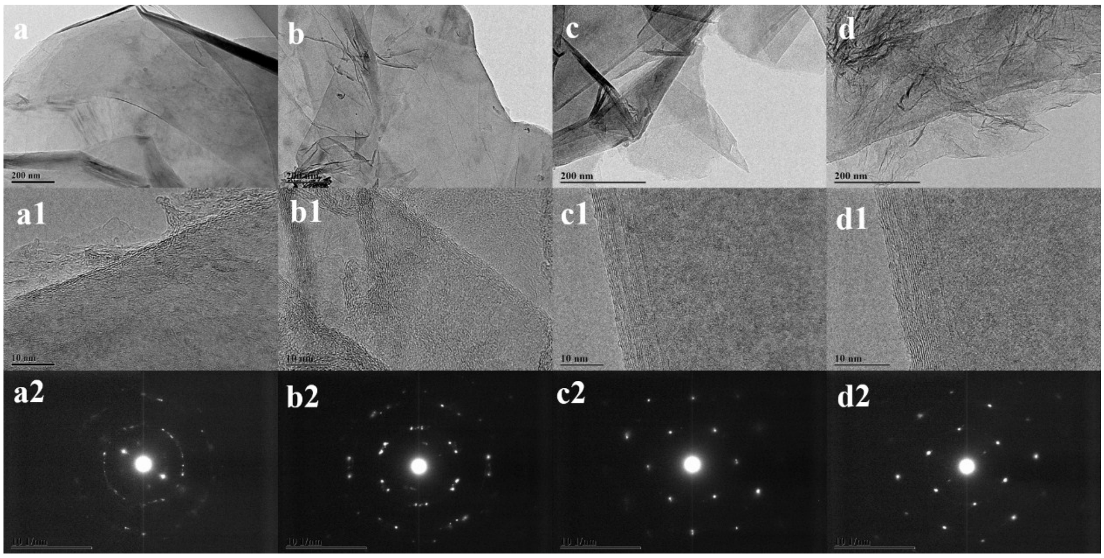

Figure S2. A-rGO650: TEM images (a), HRTEM of layer structure (a1), SAED

pattern (a2)
A-rGO800: TEM images (b), HRTEM of layer structure (b1), SAED pattern (b2)
A-rGO1000: TEM images (c), HRTEM of layer structure (c1), SAED pattern (c2)
A- rGO1100: TEM images (d), HRTEM of layer structure (d1), SAED pattern (d2)

Catalytic activity of the reference catalysts rGOT:

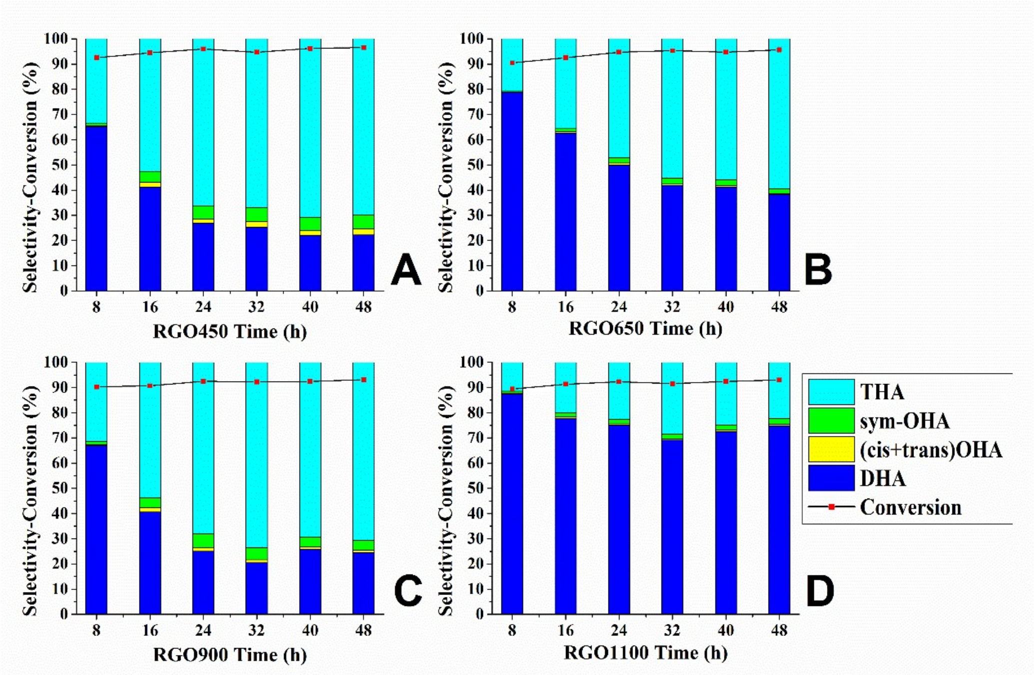

Figure S3. The anthracene conversion and hydrogenation products selectivity over rGOT. Reaction conditions: 350 °C, H_2 pressure, 4 MPa; H_2/feed: 600 cm^3/cm^3; LHSV: $2.5h^{-1}$.

The rGO were calcined at 450 °C, 650 °C, 900 °C and 1100 °C under N_2 atmosphere, respectively. The final products were named as rGOT (rGO450, rGO650, rGO900, rGO1100), in which T means the calcination temperatures.

When A-rGOT catalysts were used, higher catalytic activity was achieved e.g. more deep hydrogenation products, THA, OHA, were produced which indicate that N played an important role in the anthracene hydrogenation.

Table S2. Structure of anthracene and hydrogenation products

Anthracene	DHA	THA	*sym*-OHA	*(cis+trans)*OHA
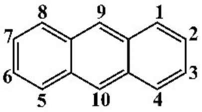	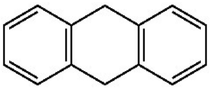	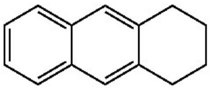	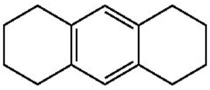	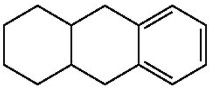

Sr values of different positions for anthracene, 1:1.073, 2:0.922, 9:1.314.

UV-vis absorption

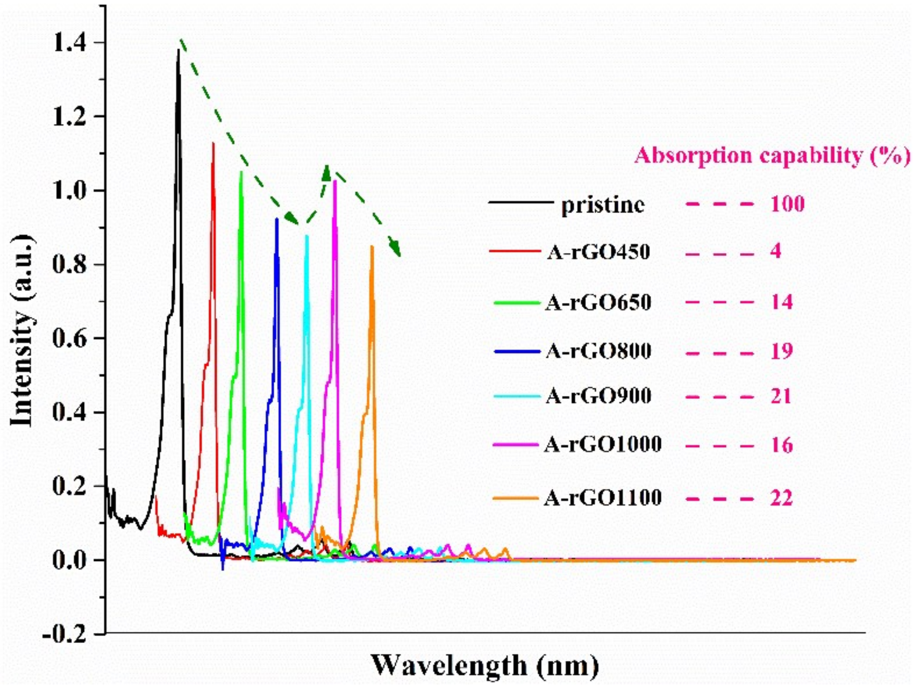

Figure S4. UV-vis absorption spectra of the substrate anthracene on A-rGO450, A-rGO650, A-rGO800, A-rGO900, A-rGO1000 and A-rGO1100 catalysts.

As stated previously, the reactant anthracene can be activated by the sp^2 carbon structure via π-π interaction. In this study, the doped N species are in the form of pyridinic N, pyrrolic N, graphitic N, and pyridine-N-oxide, in which the graphitic N (C=N) is similar to graphitic C (C=C). Because the graphitic N may enhance the π-π interaction due to the change of the graphene huge π-electron system. Thus, the ratio of graphitic N/graphitic C (C=N/C=C) may reflect the π-π interaction.

In order to verify the assumption, the UV-vis absorption experiment was designed. The A-rGO450, A-rGO650, A-rGO800, A-rGO900, A-rGO1000 and A-rGO1100 catalysts were added into the liquid feedstock (anthracene). Moreover, the feedstock were used as reference. Then the liquid samples (A-rGO450, A-rGO650, A-rGO800, A-rGO900, A-rGO1000, A-rGO1100, and reference) were characterized by UV-vis. The residual liquid feedstock concentration can reflect the π-π interaction, which was shown in Figure S4. The absorption capability was defined as (I(pristine)-I(A-rGOT))/I(pristine)*100%. (I: peak intensity from UV-vis absorption spectra)

Effect of the metallic impurities

GO was prepared with oxidation of graphite according to a modified Hummers method in which the sodium nitrate and permanganate were used as oxidant. So, the metallic impurities were qualitative analyzed by atom absorption spectrometer (AAS) and inductively coupled plasma optical emission spectroscopy (ICP-OES).

Table S3. The metallic impurities concentration of all samples from AAS.

Samples	Mn(wt%)	K(wt%)	Fe(wt%)	Na(wt%)
A-rGO450	0.240	0.034	0.023	0.013
A-rGO650	0.250	0.033	0.023	0.012
A-rGO800	0.230	0.034	0.020	0.011
A-rGO900	0.240	0.034	0.022	0.011
A-rGO1000	0.220	0.033	0.024	0.010
A-rGO1100	0.230	0.031	0.023	0.010

Table S4. The metallic impurities concentration of all samples from ICP-OES:

Samples	Mn /wt%	K /wt%	Fe /wt%	Na /wt%	Mg /wt%	Ca /wt%	Ni /wt%	Al /wt%	Zn /wt%	Cu /wt%
A-rGO450	0.230	0.033	0.024	0.014	0.0056	0.0038	0.0025	0.0015	0.0011	0.0011
A-rGO650	0.210	0.032	0.022	0.012	0.0060	0.0032	0.0029	0.0016	0.0012	0.0010
A-rGO800	0.240	0.033	0.021	0.011	0.0055	0.0033	0.0020	0.0017	0.0010	0.0011
A-rGO900	0.220	0.033	0.021	0.010	0.0050	0.0035	0.0020	0.0018	0.0011	0.0012
A-rGO1000	0.210	0.031	0.022	0.012	0.0052	0.0033	0.0022	0.0017	0.0012	0.0012
A-	0.22	0.03	0.02	0.01	0.005	0.003	0.002	0.001	0.001	0.001

rGO1100	0	2	3	1	1	7	1	8	1	0

(1) Effect of the Mn

From the results of AAS and ICP-OES, it can be seen that the major metal impurities is Mn. To exclude the influence of metal impurities Mn on the catalytic activity of A-rGOT, the feasible strategy was performed according to the report (*Nature Communications*, 2014, 5. 5291, Garcia) e.g. twice, four and twenty times of the amount of Mn were added to the catalysts.

For preparation of rGO, GO (150 mg) was dispersed in 160 mL of deionized water. The mixture was stirred for 20 min and then sonicated for approximately 20 min at room temperature. The $MnCl_2$ (0.6-7 mg) was added to the solution. Then the aforementioned solution was transferred into a 200 mL Teflon-lined autoclave, heated to 180 ^{o}C and kept for 10 h. The products denoted as reduced graphene oxide (rGO) were collected by filtered, washed with deionized water until no Cl^{-1} was detected. Then the samples were dried at 40 ^{o}C for 24 h. Subsequently, the as-synthesized rGO was treated under high purity ammonia (NH_3) atmosphere at 900 ^{o}C for 40 min, separately. The final products were denoted as Mn2-A-rGO900, Mn4-A-rGO900 and Mn20-A-rGO900 (twice, four and twenty times of the amount of Mn present in the catalysts).

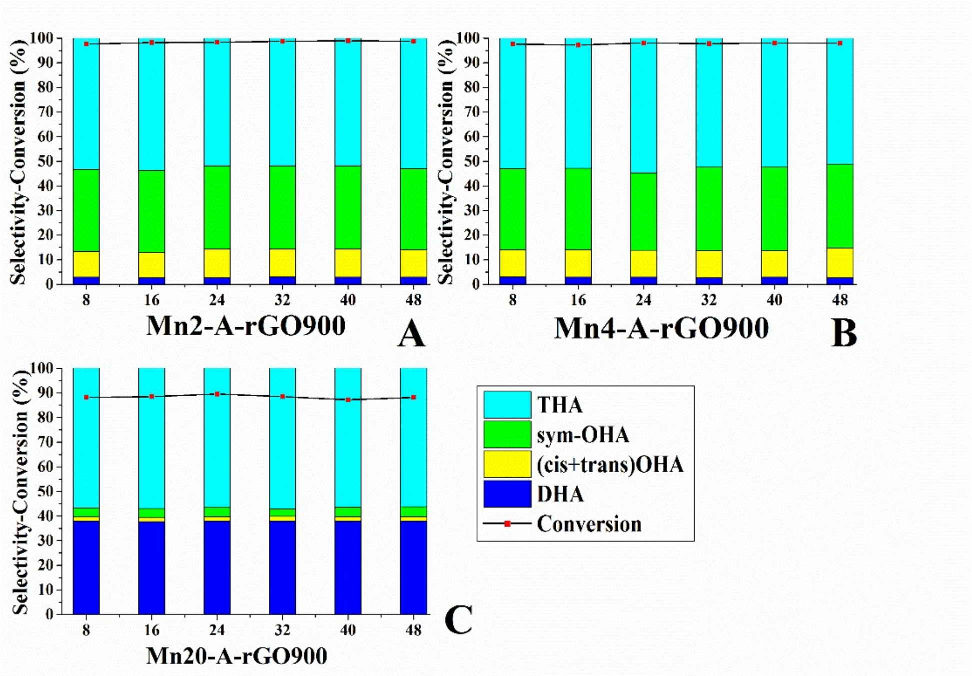

Figure S5. Anthracene hydrogenation over Mn2-A-rGO900, Mn4-A-rGO900 and Mn20-A-rGO900.

It can be found from Figure S5 that the products selectivity and anthracene conversion over Mn2-A-rGO900 and Mn4-A-rGO900 change a little compared to A-rGO900. However, when the Mn20-A-rGO900 is used as catalyst, the deep hydrogenation products OHA (*sym*-OHA, (*trans*+*cis*)OHA) and anthracene conversion decreased obviously. Thus, it can be concluded that small amount of Mn can not affect the catalytic activity of A-rGOT, and with increasing of the amount of Mn, the catalytic activity decreased. Therefore, the effect of majority metallic impurities can be excluded.

(2) Effect of the Ni

To exclude the metal impurities Ni in the catalytic activity of A-rGOT, the feasible strategy was performed according to the report (*Nature Communications*, 2014, 5. 5291, Garcia) e.g. ten, twenty, thirty and one hundred times of the amount of Ni were added to the catalysts.

For preparation of rGO, GO (150 mg) was dispersed in 160 mL of deionized water. The mixture was stirred for 20 min and then sonicated for approximately 20 min at room temperature. The $Ni(NO_3)_2 \cdot 6H_2O$ (0.16-1.5 mg) was added to the solution. Then the aforementioned solution was transferred into a 200 mL Teflon-lined autoclave, heated to 180 °C and kept for 10 h. The products denoted as reduced graphene oxide (rGO) were collected by filtered and washed with deionized water. Then the samples were dried at 40 °C for 24 h. Subsequently, the as-synthesized rGO was treated under high purity ammonia (NH_3) atmosphere at 900 °C for 40 min. The final products were denoted as N10-A-rGO900, N20-A-rGO900 N30-A-rGO900 and N100-A-rGO900 (ten, twenty, thirty and one hundred times of the amount of Ni present in the A-rGO900).

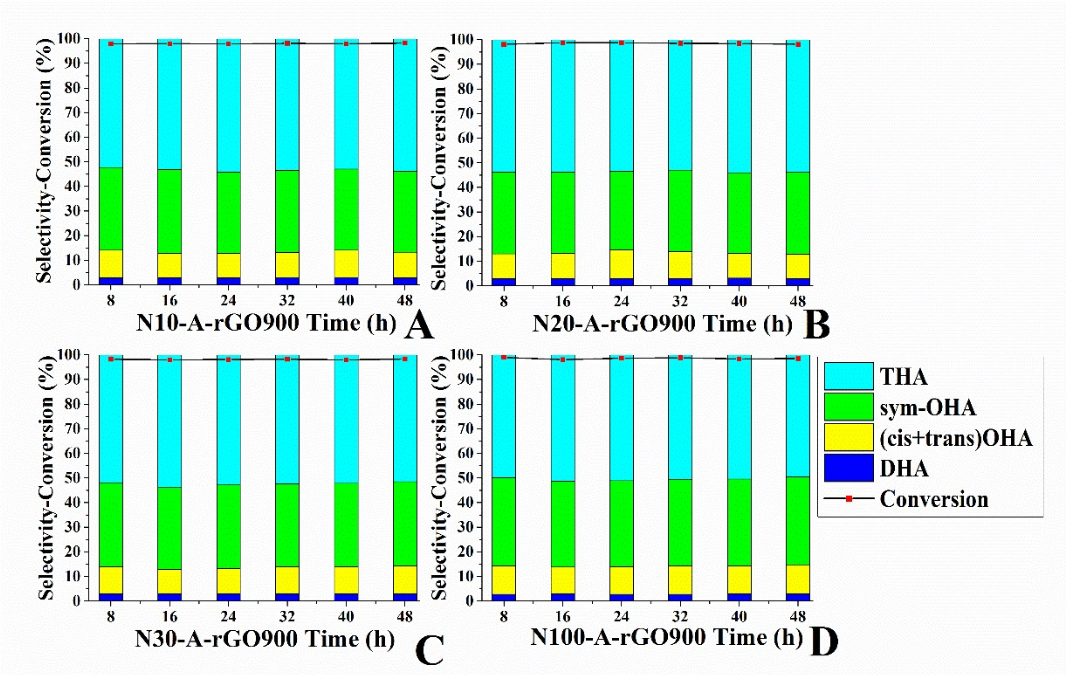

Figure S6. Anthracene hydrogenation over N10-A-rGO900 (A), N20-A-rGO900 (B), N30-A-rGO900 (C), N100-A-rGO900 (D).

It can be found from Figure S6 that the products selectivity and anthracene conversion over N10-A-rGO900, N20-A-rGO900 N30-A-rGO900 and N100-A-rGO900 change a little compared to A-rGO900. Thus, it can be concluded that small amount of Ni can not affect the catalytic activity of A-rGOT.

(3) Effect of the Cu

To exclude the metal impurities Cu in the catalytic activity of A-rGOT, the feasible strategy was performed according to the report (*Nature Communications*, 2014, 5. 5291, Garcia) e.g. ten, twenty, fifty and one hundred times of the amount of Cu were added to the catalysts.

For preparation of rGO, GO (150 mg) was dispersed in 160 mL of deionized water. The mixture was stirred for 20 min and then sonicated for approximately 20 min at room temperature. The $Cu(NO_3)_2 \cdot 3H_2O$ (0.07-0.8 mg) was added to the solution. Then the aforementioned solution was transferred into a 200 mL Teflon-lined autoclave, heated to 180 °C and kept for 10 h. The products denoted as reduced graphene oxide (rGO) were collected by filtered and washed with deionized water. Then the samples were dried at 40 °C for 24 h. Subsequently, the as-synthesized rGO was treated under high purity ammonia (NH_3) atmosphere at 900 °C for 40 min. The final products were denoted as C10-A-rGO900, C20-A-rGO900, C50-A-rGO900 and C100-A-rGO900 (ten, twenty, fifty and one hundred times of the amount of Cu present in the A-rGO900).

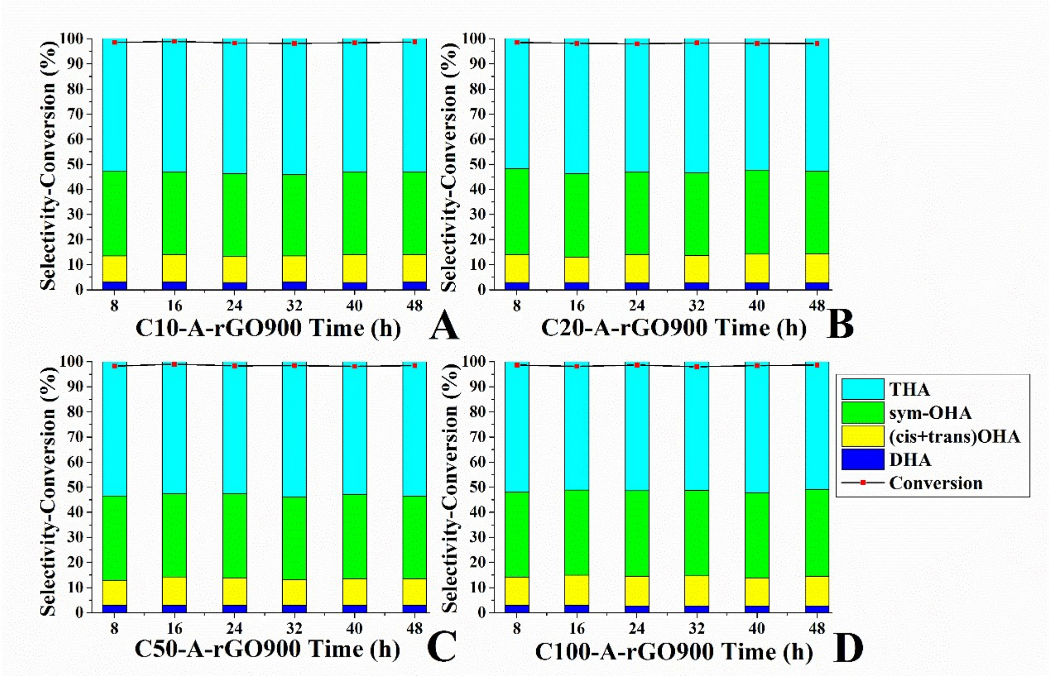

Figure S7. Anthracene hydrogenation over C10-A-rGO900 (A), C20-A-rGO900 (B), C50-A-rGO900 (C) and C100-A-rGO900 (D).

It can be found from Figure S7 that the products selectivity and anthracene conversion over C10-A-rGO900, C20-A-rGO900, C50-A-rGO900 and C100-A-rGO900 change a little compared to A-rGO900. Thus, it can be concluded that small amount of Cu can not affect the catalytic activity of A-rGOT.

The stability test

The catalyst A-rGO900 was tested to study the stability for anthracene hydrogenation. The result showed that the anthracene conversion and the products selectivity were almost invariable for 336h (Figure S8).

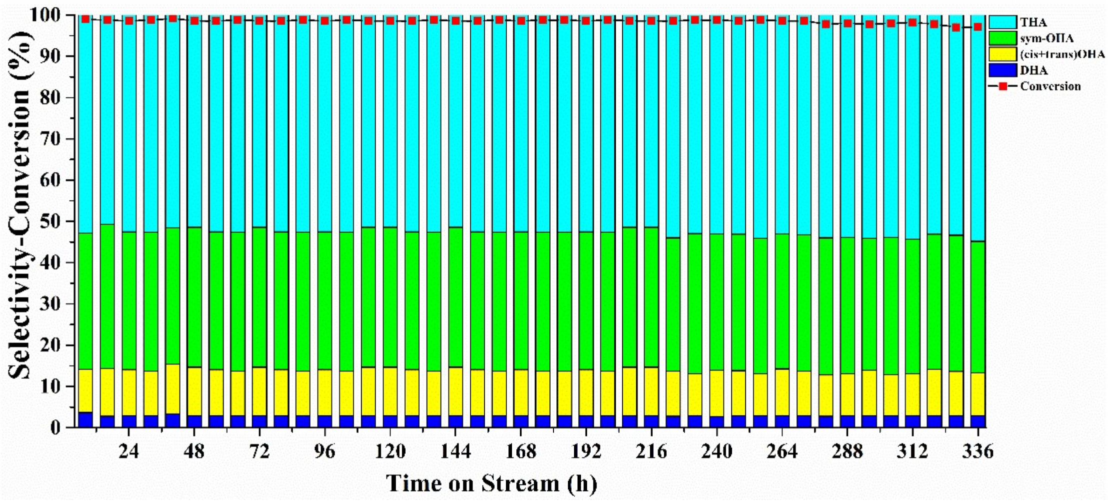

Figure S8. Products selectivity and anthracene conversion over A-rGO900. Reaction conditions: 350 °C, H_2 pressure, 4MPa; H_2/feed : 600 cm^3/cm^3; LHSV: 2.5h^{-1}.

Stability of N

(1) The exit gas was analyzed by mass spectrometer (MS) as shown in Figure S9. From the result, it can be seen that no NH_3 were detected in the outlet gas over A-rGOT catalysts.

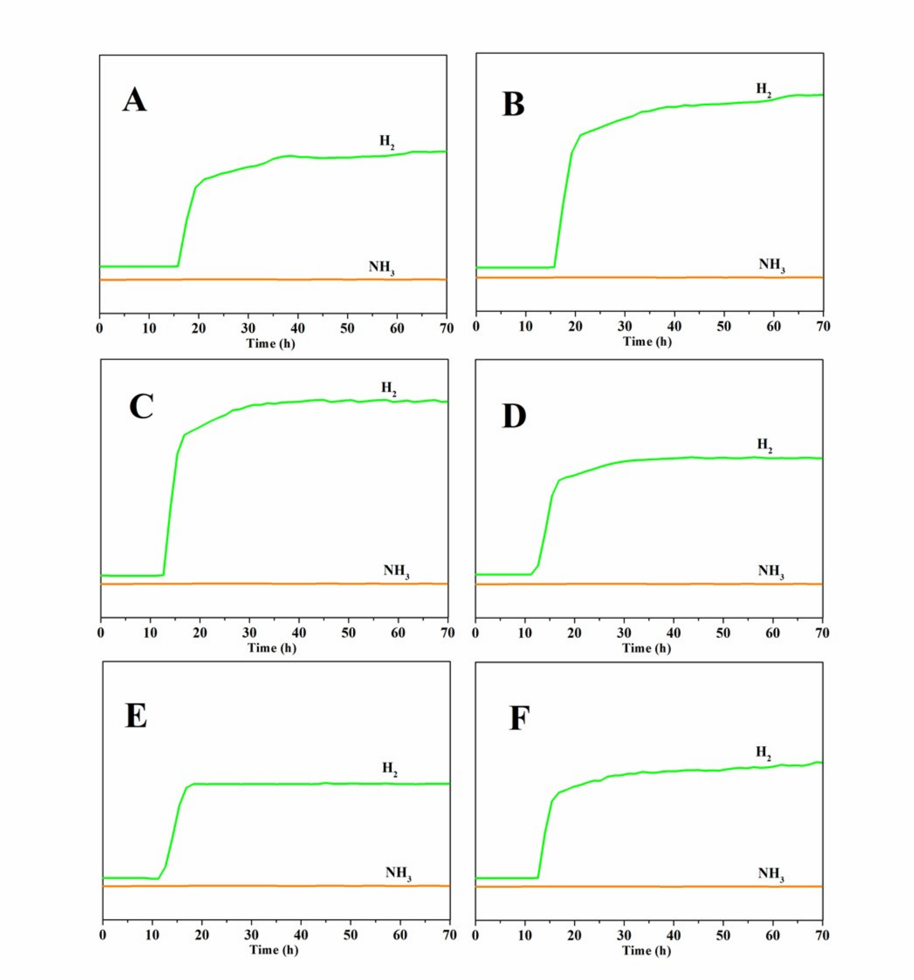

Figure S9. The outlet gas of anthracene hydrogenation reaction over A-rGO450 (A), A-rGO650 (B) A-rGO800 (C), A-rGO900 (D), A-rGO1000 (E), A-rGO1100 (F).

(2) The used catalysts were also characterized by XPS.

Table S5. Atomic percentage of the samples derived from XPS

Sample	C (at%)		N (at%)		O (at%)	
	fresh	used	fresh	used	fresh	used
A-rGO450	85.21	85.42	7.62	7.57	7.17	7.01
A-rGO650	87.87	88.87	6.62	6.65	5.51	4.48
A-rGO800	93.05	92.98	5.28	5.31	1.67	1.71
A-rGO900	95.15	94.74	3.67	4.19	1.18	1.07
A-rGO1000	96.34	96.38	2.76	2.77	0.90	0.85
A-rGO1100	97.92	98.02	1.62	1.65	0.46	0.33

From the results of XPS (Table S5), it can be seen that the nitrogen contents were nearly unchanged compared to the fresh catalysts which indicate that the doped N is stable. For oxygen, the C–OH, COOH, and C-O-C groups were formed which were unstable in the hydrogenation reaction.

Catalytic performance at high GHSV of H_2

The anthracene hydrogenation over A-rGOT with increasing of the GHSV of H_2 (67.5 ml/min) is shown in Figure S10. The anthracene conversion decrease to about 90%. While the products selectivities are similar to that of the GHSV of H_2 (45 ml/min).

The anthracene hydrogenation over A-rGOT with increasing of the GHSV of H_2 (135 ml/min) is shown in Figure S11. The anthracene conversion are about 70% while the deep hydrogenation products OHA decrease remarkably.

The anthracene hydrogenation over A-rGOT with increasing the GHSV of H_2 (180 ml/min) is shown in Figure S12. The anthracene conversion decrease to about 60% and the differences between selectivities are not obviously.

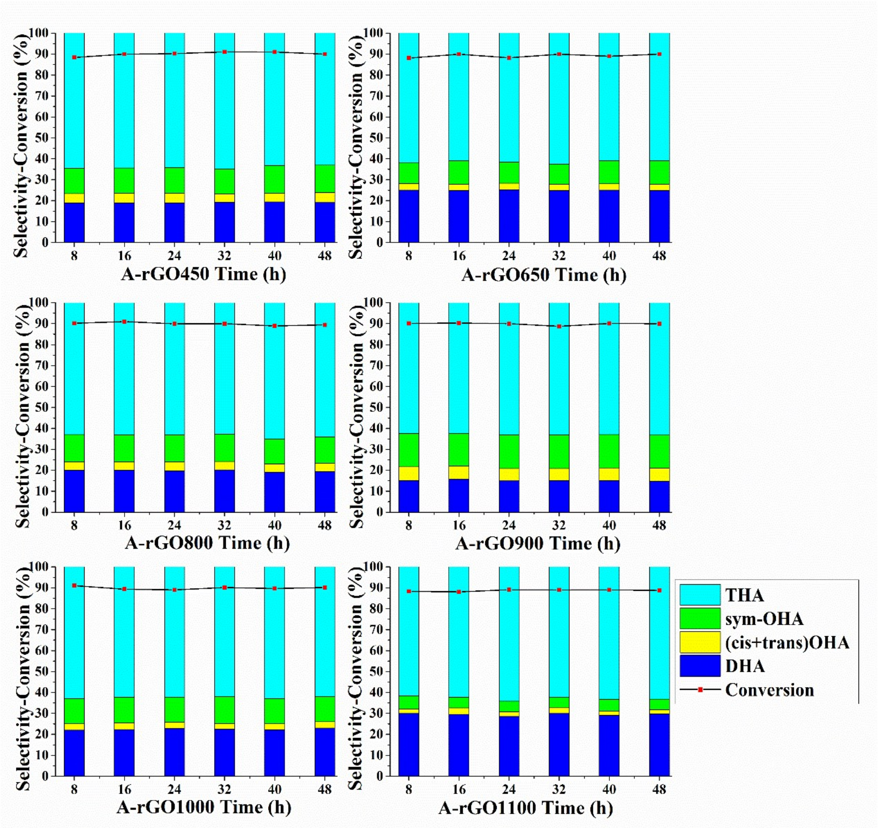

Figure S10. Anthracene conversion and products selectivity over A-rGO450, rGO650, A-rGO800, rGO900, A-rGO1000 and A-rGO1100. Reaction conditions: 350 ^{o}C, H_2 pressure, 4MPa; H_2/feed: 600 cm^3/cm^3; H_2 67.5 mL/min.

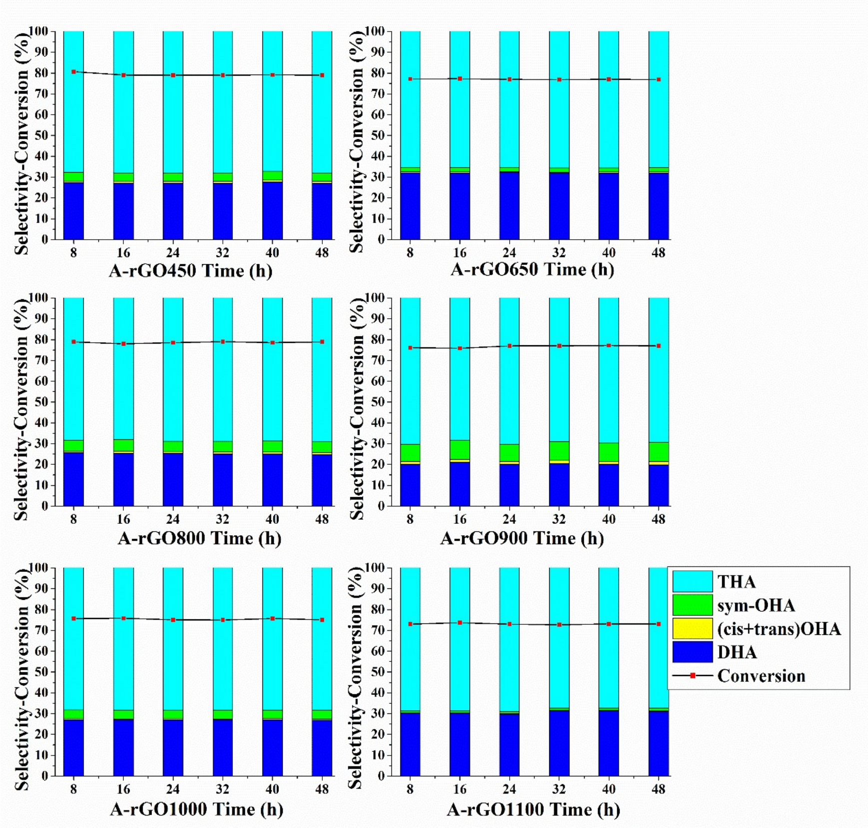

Figure S11. Anthracene conversion and products selectivity over A-rGO450, rGO650, A-rGO800, rGO900, A-rGO1000 and A-rGO1100. Reaction conditions: 350 ^{o}C, H_2 pressure, 4MPa; H_2/feed: 600 cm^3/cm^3; H_2 135 mL/min.

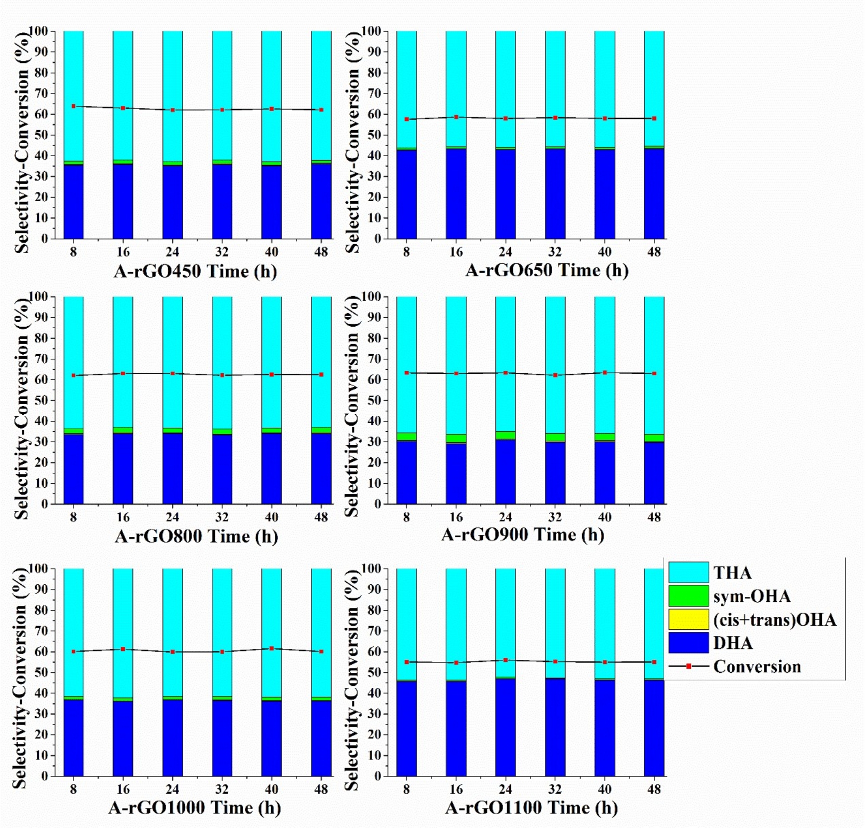

Figure S12. Anthracene conversion and products selectivity over A-rGO450, rGO650, A-rGO800, rGO900, A-rGO1000 and A-rGO1100. Reaction conditions: 350 ^{o}C, H_2 pressure, 4MPa; H_2/feed: 600 cm^3/cm^3; H_2 180 mL/min.